fermentation

MDPI

Article

Bioconversion of Agro-Industrial Byproducts Using *Bacillus* sp. CL18: Production of Feather Hydrolysates for Development of Bioactive Polymeric Nanofibers

Naiara Jacinta Clerici [1], Daniel Joner Daroit [2], Aline Aniele Vencato [1] and Adriano Brandelli [1,*]

[1] Laboratory of Nanobiotechnology and Applied Microbiology, Institute of Food Science and Technology, Federal University of Rio Grande do Sul, Av. Bento Gonçalves 9500, Porto Alegre 91501-970, Brazil; naiaraj.clerici@gmail.com (N.J.C.); aline_vencato@hotmail.com (A.A.V.)

[2] Postgraduate Program in Environment and Sustainable Technologies, Campus Cerro Largo, Federal University of Fronteira Sul, Av. Jacob Reinaldo Haupenthal 1580, Cerro Largo 97900-000, Brazil; daniel.daroit@uffs.edu.br

* Correspondence: abrand@ufrgs.br

Abstract: Microbial fermentation represents an interesting strategy for the management and valorization of agro-industrial byproducts. In this study, the proteolytic strain *Bacillus* sp. CL18 was used to produce bioactive hydrolysates during submerged cultivation with various protein-containing substrates, including byproducts from the poultry (feathers), cheese (whey), fish (scales), and vegetable oil (soybean meal) industries. The bioactive feather hydrolysates (BFHs) showing high antioxidant activity were incorporated in poly(vinyl alcohol) (PVA) and poly-ε-caprolactone (PCL) nanofibers by the electrospinning technique. The PVA nanofibers containing 5% BFH reached antioxidant activities of 38.7% and 76.3% for DPPH and ABTS assays, respectively. Otherwise, the PCL nanofibers showed 49.6% and 55.0% scavenging activity for DPPH and ABTS radicals, respectively. Scanning electron microscopy analysis revealed that PVA and PCL nanofibers containing BFH had an average diameter of 282 and 960 nm, respectively. Moreover, the results from thermal analysis and infrared spectroscopy showed that the incorporation of BFH caused no significant modification in the properties of the polymeric matrix. The bioconversion of feathers represents an interesting strategy for the management and valorization of this byproduct. Furthermore, the effective incorporation of BFH in polymeric nanofibers and validation of the biological activity suggest the application of these materials as antioxidant coatings and packaging.

Keywords: agro-industrial byproduct; antioxidant activity; bioactive potential; fermentation; keratinolysis; polymeric nanofibers

Citation: Clerici, N.J.; Daroit, D.J.; Vencato, A.A.; Brandelli, A. Bioconversion of Agro-Industrial Byproducts Using *Bacillus* sp. CL18: Production of Feather Hydrolysates for Development of Bioactive Polymeric Nanofibers. *Fermentation* **2024**, *10*, 615. https://doi.org/10.3390/fermentation10120615

Academic Editor: Yusuf Chisti

Received: 15 October 2024
Revised: 26 November 2024
Accepted: 28 November 2024
Published: 30 November 2024

1. Introduction

Enormous amounts of waste and byproducts are inevitably generated by agro-industrial activities in the course of food production. Soybean meal, for instance, is the major byproduct of oilseed processing, with an estimated amount of 247 million tons produced annually [1]. This protein-rich material is usually directed to animal feed and is also employed to obtain protein isolates for food applications [1,2]. Whey is the most abundant byproduct from the cheese and casein industries, reaching around 200 million tons. It may be employed as fertilizer and animal feed, but only half of the produced whey is further processed to obtain proteins, lactose, and minerals as added-value products [3].

Several byproducts also originate from slaughterhouses. For instance, nearly 60% of a fish's live weight is commonly discarded from the fileting process. Fish scales represent about 5% of generated byproducts, from which collagen might be extracted [4]. Byproducts from broiler processing reach approximately 40% of their live weight. Feathers are keratin-rich and recalcitrant byproducts representing 5–10% of broiler weight, which amounts to a

global production of approximately 5 million tons per year. Currently, feathers are mainly converted into feather meal through hydrothermal treatments for use as animal feed [5].

In this scenario, the management of residual biomasses remains a relevant challenge that is related not only to the environmental and health burdens of improper disposal but also (and especially) the search for upcycling alternatives [6]. Additionally, it should be considered that agriculture and animal production are resource-intensive activities; thus, the utilization of processing byproducts might also contribute to minimizing the impacts on natural resources, thus providing a robust framework for sustainable development [7]. Microbial processes are notably relevant for the eco-friendly valorization of agri-food byproducts, which is vital for circular economies [8]. Composting, for instance, is an important strategy for sustainable agriculture [9], and the production of biogas and bioethanol play expanding roles in energy security [10]. In addition, microbial technologies might provide a wide array of valuable biomolecules with commercial and industrial significance [6].

Increasing attention has been drawn to the release of antioxidant molecules from diverse substrates through fermentations, as in the case of soybean meal or soy protein isolate fermented with *Bacillus subtilis* [11,12]. Cultivations with different bacterial strains augmented the bioactive potential of milk-derived substrates through the release of antioxidant peptides from caseins and whey proteins [13,14]. Microbial processing of slaughterhouse wastes also holds promise in this regard. Antioxidant hydrolysates were produced from the bioconversion of feathers by *Bacillus* sp. TC5 [15] and *Ochrobactrum intermedium* [16]. The fermentation of fishery byproducts has also been demonstrated as an interesting approach to release antioxidants. Moreover, the generation of antioxidant hydrolysates during the bioprocessing of mixed fish wastes with *Yarrowia lipolytica* YL2 has been reported [17]. Increased antioxidant activities were also demonstrated for fish skin wastes fermented by *Bacillus subtilis* L4 [18].

Antioxidants recovered from fermentations are postulated for use in cosmetics, pharmaceuticals, and food additives due to their health-benefiting effects and preservative properties [19]. More recently, nanotechnology came into play, expanding the applicability of antioxidant compounds [20]. The incorporation of antioxidants into nanostructures, for instance, might be an adequate strategy to increase the stability and biocompatibility of such bioactives, also permitting their controlled release and delivery. Such materials find applications in food packaging, wound healing, tissue regeneration, and engineering, among others [21]. Electrospinning is a promising technique for manufacturing nanofibers with a large surface-to-volume ratio and good mechanical and thermal properties. For example, nanofibers can be used to incorporate a high amount of bioactive compounds to develop functional materials for active packaging and drug delivery [22–24]. However, the electrospinning of bioactive protein hydrolysates obtained from bioprocesses has been the subject of a few studies. For example, bioactive casein hydrolysates produced by enzymatic catalysis using commercial enzymes could be incorporated into pullulan-based electrospun nanofibers [25]. In another study, the hydrolysates obtained from the microbial bioprocessing of keratin were successfully employed in the formulation of PCL nanofibers via electrospinning [26]. Thus, the research on microbial conversion of agro-industrial byproducts for the development of innovative nanomaterials may represent a benefit to the field by addressing sustainability issues and the valorization of wastes.

Bacillus sp. CL18 is a proteolytic bacterium isolated from soil, showing the ability to produce hydrolysates with outstanding biological activities [27,28]. In this work, the objective was to investigate the antioxidant potential of protein hydrolysates produced by this strain and their incorporation into nanofibers. In this context, feather hydrolysates with high antioxidant activity, obtained by bioprocessing with the strain CL18, were used to manufacture nanofibers using two different biocompatible polymers, poly(vinyl alcohol) (PVA) and poly-ε-caprolactone (PCL). The incorporation of bioactive feather hydrolysates (BFHs) resulted in functionalized nanofibers with biological activity. In addition, the thermal, mechanical, and structural characterization of BFH nanofibers was performed.

2. Materials and Methods

2.1. Chemicals

Poly(vinyl alcohol) (PVA; average MW 85,000–124,000, 87–89% hydrolyzed), poly-ε-caprolactone (PCL; average MW 80,000 Da), 2,2-diphenyl-1-picrylhydrazyl (DPPH), 2,2′-azino-bis-(3-ethylbenzothiazoline)-6-sulfonic acid (ABTS), and 6-hydroxy-2,5,7,8-tetramethylchroman-2-carboxylic acid (Trolox) were obtained from Sigma Aldrich (St. Louis, MO, USA). Tetrahydrofuran (THF) and N-dimethylformamide (DMF) were obtained from Merck (Darmstadt, Germany). Sodium chloride (NaCl), monopotassium phosphate (KH_2PO_4), and calcium chloride ($CaCl_2$) were acquired from Labsynth (São Paulo, Brazil). All other reagents used were of analytical grade and all solutions were prepared with distilled water.

2.2. Microorganism and Inoculum Preparation

Bacillus sp. CL18 was routinely maintained in Agar Brain Heart Infusion (BHI) plates at 7 °C. The previously characterized strain CL18 [27] was retrieved from the culture collection of Laboratory of Applied Microbiology (UFFS, Cerro Largo, Brazil). To prepare the inoculum for submerged cultivations, the bacterium was streaked onto fresh BHI plates and incubated at 30 °C for 24 h. Thereafter, the bacterial biomass was aseptically collected and added to sterile saline (8.5 g/L NaCl) to reach ~1.0 absorbance unit at 600 nm. The obtained cell suspensions were used as inoculum.

2.3. Submerged Cultivations of Bacillus sp. CL18 in Different Substrates

Submerged cultivation (SmF) was carried out in 250 mL Erlenmeyer flasks containing 50 mL of mineral medium (0.5 g/L NaCl, 0.3 g/L K_2HPO_4, 0.4 g/L KH_2PO_4, pH 7.0), and one of the following substrates (10 g/L): casein (Synth, São Paulo, Brazil), soy protein isolate (SPI; Bunge Alimentos, Esteio, Brazil), soybean meal (SBM; Warpol Agroindustrial, Guarani das Missões, Brazil), whey protein isolate (WPI; Alibra Ingredientes, Campinas, Brazil), lyophilized sweet whey (LSW; whey from Laticinios Konzen, Cerro Largo, Brazil) obtained by freeze-drying in a LS3000D lyophilizer (Terroni, São Carlos, Brazil), fish scales (obtained from local fishermen), whole feathers (white chicken feathers, ~6–8 × 1.5–2.5 cm, collected from local slaughterhouse), and milled white feathers processed in an analytical mill (IKA® A11, Staufen, Germany).

After autoclave sterilization (121 °C, 15 min) and cooling, flasks were inoculated with 1 mL of the bacterial suspension and incubations were performed at 30 °C, 125 rpm from 0 to 7 days. Triplicate flasks were withdrawn every 24 h, and the media were centrifuged (10,000× *g*, 20 min) to collect the supernatants, which were then boiled (5 min). Evaluations involved the determination of soluble protein contents through the Folin-phenol method [29] and the radical-scavenging activity using the ABTS assay [30], as detailed below. The proteolytic activity was also monitored during SmF in whole feathers using azocasein (Sigma Aldrich) as substrate, as described previously [28].

2.4. Production of Bioactive Feather Hydrolysate (BFH)

Feathers were carefully cleaned and soaked in a 1:1 (*w*/*v*) ratio of chloroform–methanol to remove stains or any grease residue. Clean feathers were cut and added (10 g/L) to the mineral medium. After autoclave sterilization, media were inoculated, and submerged cultivations were carried out at 30 °C, 125 rpm for 120 h. Subsequently, culture supernatants were centrifuged (10 min, 10,000× *g*, 4 °C), frozen, lyophilized [28], and then used for production of nanofibers.

2.5. Nanofibers Manufacturing

PCL was dissolved using a 1:1 (*v*/*v*) ratio of THF:DMF, and PVA was dissolved in distilled water, both at concentrations of 10% (*w*/*v*) and 15% (*w*/*v*). BFH was mixed with polymer solutions at three concentrations (1, 2.5, and 5% based on polymer weight) to generate different electrospinning solutions (ESs). For the electrospinning process, a

syringe containing 3 mL of ES was coupled to an electrospinner (BR Robotics, Porto Alegre, Brazil). The following processing conditions were applied: voltage of 20 kV; feeding rate of 0.08 mL/min; needle inner diameter 0.5 mm; distance to collector 15 cm. The process was performed at 25 °C. The nanofibers were collected on an aluminum plate (15 × 15 cm) and dried overnight to eliminate residual solvent.

2.6. Biological Activities of Nanofibers

2.6.1. Antioxidant Activity

The antioxidant potential of the nanofibers was evaluated through the scavenging of 2,2-diphenyl-1-picrylhydrazyl (DPPH) [31] and 2,2′-azinobis-(3-ethylbenzothiazoline-6-sulfonic acid) (ABTS) radicals [30]. Trolox solutions (concentration range 0.1–2.0 mM) were prepared to construct analytical curves for the expression of antioxidant activities as the Trolox equivalent (TEAC).

The initial test on the antioxidant potential of nanofibers was carried out using the DPPH radical previously diluted in methanol using 5 mg of carefully weighed nanofibers. For this experiment, the capture of free radicals was monitored over time at pre-established incubation periods of 0.5, 24, 40, and 48 h.

The second block of experiments for antioxidant activities was performed using an extraction protocol, suggested with the aim of releasing the peptides responsible for the bioactivity [32]. Subsequently, the DPPH activity was investigated again over an incubation period of 1 h [31], and the ABTS scavenging activity was performed according to standard methodology [30].

For both experiments, the results were expressed in terms of percentage of scavenging activity using the following formula:

$$\text{Scavenging (\%)} = [(A_{control} - A_{sample})/A_{control}] \times 100 \quad (1)$$

2.6.2. Hemolytic Activity

The nanofibers were weighed (4 mg), added to 1 mL PBS (pH 7.4), and then mixed with 1 mL of erythrocyte suspension (4%, *v*/*v*). The samples were incubated for 60 min at 37 °C and then centrifuged at 3000 *g* for 10 min. An aliquot (1 mL) of the supernatant was removed for absorbance reading at 540 nm. Hemolytic activity was determined with the following equation:

$$\text{Hemolytic activity (\%)} = (AS - AN)/(AP - AN) \times 100\% \quad (2)$$

where AS is the supernatant reading, AN is the negative control, and AP is the positive control. Triton X-100 (0.1%, *v*/*v*) and PBS were used as positive and negative controls, respectively [33].

2.7. Physicochemical and Structural Characterization of Nanofibers

2.7.1. Scanning Electron Microscopy (SEM)

The nanofibers were metalized with gold coating, and the morphology of the nanofiber membranes was examined by scanning electron microscopy (Zeiss EVO MA10, Oberkochen, Germany). Histograms presented here were acquired through the measurement of at least 100 nanofibers, coming from several images obtained through SEM, analyzed in at least four different regions of the material surface.

2.7.2. Thermal Analyses

The thermogravimetric analysis (TGA) was performed using a model Pyris 1 TGA (Perkin Elmer, CA, USA). Samples were heated in platinum pans from 25 to 800 °C at a rate of 10 °C/min under a nitrogen atmosphere (flow rate of 20 mL/min).

Differential scanning calorimetry (DSC) studies were performed using a DSC 8500 apparatus (Perkin Elmer, CA, USA). Samples equivalent to approximately 11 mg were

placed in aluminum pans and heated from 20 to 200 °C, with a heating rate of 10 °C/min under a nitrogen flow of 20 mL/min.

2.7.3. Fourier Transform Infrared Spectroscopy (FTIR)

The spectrum was obtained by the ATR method using a Perkin Elmer Spectrum IR Version 10.7.2 in the region between 4000 and 500 cm^{-1} with 8 scans and resolution of 4 cm^{-1}.

2.7.4. Mechanical Analysis

The mechanical properties of the nanofibers, including tensile strength and elongation at break, were determined using a microcomputer-controlled texture analyzer model TA.XT PLUS (Stable Micro Systems, Godalming, UK). In accordance with ASTM D638, a strain rate of 10 mm/min and a clamping distance of 40 mm were used throughout the experiment. The nanofibers were cut into 50 × 10 mm samples. Tests were replicated three times for each sample.

2.8. Statistical Analysis

For the experiments on biological activity and mechanical analyses, values were expressed as the means ± standard deviation of three experiments. Comparisons between means were performed through analysis of variance and, if differences were significant, means were compared through Tukey's test ($p < 0.05$).

3. Results and Discussion

3.1. Soluble Protein and Antioxidant Activity During SmF

Bacillus sp. CL18 was cultivated on different protein-rich substrates and the soluble protein content and antioxidant activity were monitored during SmF. The soluble protein concentration remained relatively stable during cultivations with *Bacillus* sp. CL18 in casein-, LSW-, and SBM-based media compared to the respective initial values (day 0), whereas a decreasing trend was noticed in media containing fish scales. Contrarily, increases were detected in media formulated with SPI, WPI, feathers, and feather meal (Figure 1A). The greatest soluble protein increases were observed with whole feathers, from 0.05 mg/mL (day 0) to 4.87 mg/mL (day 5), and with milled feathers, from 0.29 mg/mL (day 0) to 5.31 (day 5). The hydrolysis of these protein-rich substrates with the subsequent release of soluble protein is compatible with the proteolytic potential of *Bacillus* sp. CL-18 [27]. The production of proteolytic enzymes was monitored during SmF on whole feathers, reaching maximum values of about 800 U/mL at day 5 (Supplementary Figure S1).

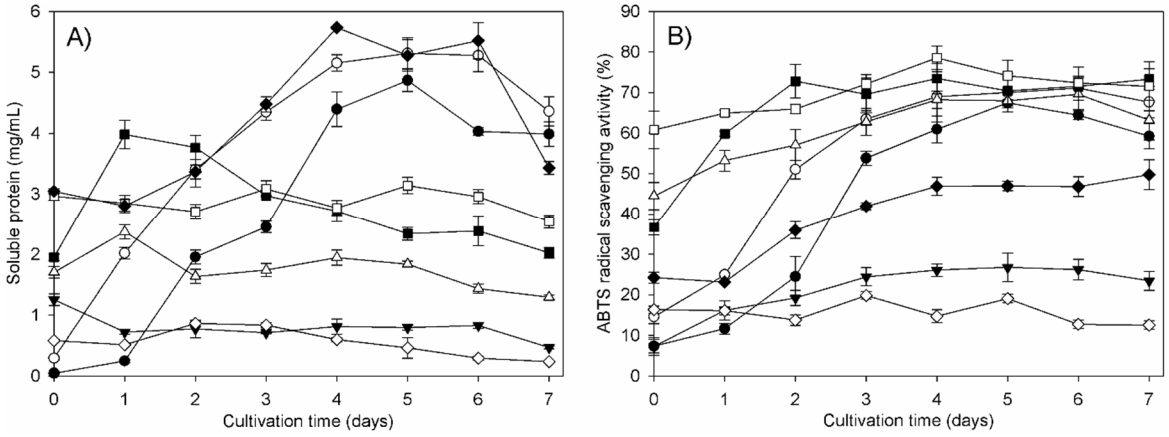

Figure 1. Soluble protein contents (**A**) and ABTS radical-scavenging activity (**B**) during submerged cultivations with *Bacillus* sp. CL18 in media containing whole feathers (●), milled feathers (○), fish scales (▼), soybean meal (SBM, △), soy protein isolate (SPI, ■), casein (□), whey protein isolate (WPI, ◆), and lyophilized sweet whey (LSW, ◇).

Regarding antioxidant activities, the ability to scavenge ABTS radicals was higher in all culture supernatants compared to the beginning of cultivations, except for the LSW-based medium. Specifically, the radical-scavenging abilities after 4 days of SmF were 78.6, 68.2, 26.0, 73.5, and 46.0% in supernatants of casein, SBM, fish scales, SPI, and WPI media, respectively, compared to the initial values of 60.8, 44.5, 7.3, 36.6, and 24.2% (Figure 1B). However, higher increments of antioxidant activities were detected in the whole-feather medium, which increased from 7.4% (day 0) to 67.5% (day 5), and in the milled-feather medium, which was augmented from 14.6% (day 0) to 70.1% (day 5).

SmF was postulated as a strategy for the bioconversion of various protein-containing substrates, including commercially valuable protein sources (WPI, SPI, casein) and byproducts from the poultry (feathers), cheese (LSW), fish (scales), and vegetable oil (SBM) industries. Through this approach, microbial enzymes could hydrolyze macromolecules to release bioactive compounds [19]. For instance, the extracellular proteases produced by *Bacillus* sp. CL18 during growth with these substrates [34] would result in amino acids and bioactive peptides, which might subsequently be recovered from culture media. The higher antioxidant activities observed during cultivations with *Bacillus* sp. CL18 reinforce that such a phenomenon indeed occurred. In this context, the bioactive peptides released upon protein hydrolysis are the major antioxidants recovered during microbial cultivations using substrates from animal sources [19]. This might also apply to SPI, as soybean proteins are highly concentrated (>90% protein). In the case of SBM, even though bioactive peptides might have been released, it should be noted that phenolic compounds found in plant biomasses could be the main determinants of antioxidant activities [35].

Complementarily, the soluble protein contents of culture supernatants were not always positively correlated with radical-scavenging abilities (Figure 1). In this scenario, and with the possible exception of SBM (due to phenolic acids/flavonoids), it is suggested that the properties of the released peptides, including their sizes and amino acid sequences, were responsible for the increased antioxidant activities observed during cultivations [36]. For highly soluble protein substrates, such as casein, SPI, and WPI, enzymatic hydrolysis might be better suited for the efficient production of antioxidant hydrolysates, while microbial processing gains momentum regarding the use of abundant and structurally complex agro-industrial byproducts [37]. In our study, byproducts were the most promising sources of antioxidant hydrolysates, particularly chicken feathers. In fact, an extensive biodegradation of feathers could be observed after SmF with *Bacillus* sp. CL18 (Figure 2). The culture supernatant obtained after feather hydrolysis by strain CL18 was analyzed by SDS-PAGE, revealing a broad molecular weight range of soluble proteins, including peptides with less than 10 kDa (Supplementary Figure S2). This indicates that several peptides are released during feather biodegradation by *Bacillus* sp. CL18. In parallel with the increased antioxidant activity observed during cultivation, this agrees with the fact that the main antioxidants obtained during microbial growth on animal byproducts are peptides released from these protein-rich substrates [14–19].

Proper management of keratin-rich byproducts remains a relevant challenge due to both its recalcitrance and the enormous amounts generated worldwide [5]. Therefore, the use of feathers as a substrate in SmF could be an appropriate biorefining strategy focusing on environmental and industrial sustainability, allowing for the cost-effective and simultaneous production of valuable products, including antioxidants and microbial enzymes [37]. Bioactive feather hydrolysates (BFHs) are envisaged for utilization by the food, feed, cosmetics, pharmaceuticals, and other industries [5]. However, the incorporation of such antioxidant hydrolysates into nanostructures is scarcely reported [26]; therefore, efforts in this direction might pave the way to create innovative biomaterials with relevant applications. Since SmF with whole feathers was effective in yielding antioxidant hydrolysates without the need for upstream processing (milling), hydrolysates obtained with this substrate were selected for nanofiber development.

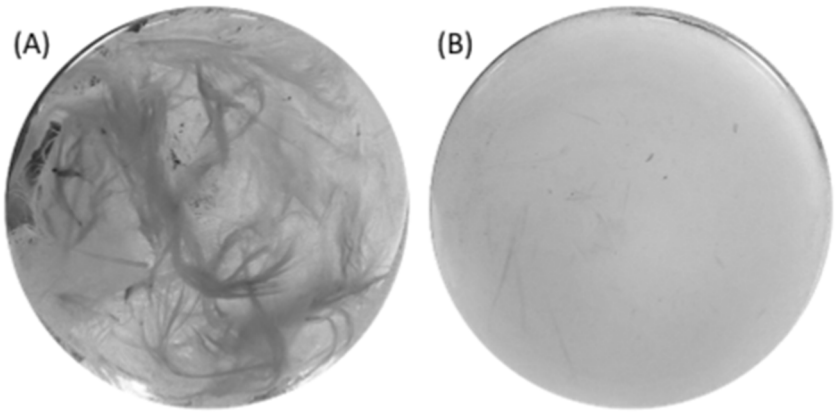

Figure 2. Feather degradation by *Bacillus* sp. CL18. Bottom views of Erlenmeyer flasks containing mineral medium and feathers (10 g/L), incubated with *Bacillus* sp. CL18 for (**A**) 0 h and (**B**) 120 h (5 days).

3.2. Antioxidant Activity of Nanofibers

Nanofibers incorporating BFH in both PVA and PCL matrixes were successfully obtained by electrospinning. These nanostructures were initially tested directly for the scavenging of the DPPH radical. For the nanofibers produced using PVA, it was noted that the addition of BFH directly interfered with the antioxidant activity over time, that is, the highest the BFH quantity and the highest the activity (Supplementary Table S1). As for nanofibers composed of PCL, there was not such a strong relationship between the increase in BFH concentration and the antioxidant activity (Supplementary Table S2). Even so, it was observed that the maximum DPPH scavenging activity occurred after 24 h, suggesting that the antioxidant peptides were strongly entrapped in the nanofiber matrix. In agreement with the data presented here, the same bioactive time release behavior has been observed for PVA/gelatin nanofiber membranes [38].

Furthermore, a buffer extraction process was employed to assist the release of antioxidant activity from the nanofibers [32]. The results are summarized in Table 1. The DPPH scavenging activity of the extracts after 1 h incubation was similar to that observed for the nanofibers directly in contact with the DPPH solution for 24 h. Thus, it was possible to note that the nanofibers manufactured with PCL had more activity for this test than the nanofibers made with PVA, reaching the maximum activity of 49%. The ABTS test also showed elevated values of antioxidant activity for formulations containing 5% BFH, reaching 1213 µM TEAC (55% inhibition) and 1694 µM TEAC (76% inhibition) for PCL and PVA nanofibers, respectively (Table 1). Regarding the activity using the ABTS radical method, the more BFHs added, the greater the free radical inhibitory activity.

Table 1. Antioxidant properties of poly-ε-caprolactone (10% PCL) and poly(vinyl alcohol) (10% PVA) nanofibers [1].

Nanofiber	DPPH (%)	DPPH (µM) [2]	ABTS (%)	ABTS (µM) [2]
PCL (control)	nd [3]	nd	nd	nd
PCL + 1% BFH	48.7 ± 1.0	967.7 ± 12.5 [a]	50.8 ± 1.4	1118.7 ± 31.1 [b]
PCL + 2.5% BFH	49.4 ± 0.6	977.7 ± 6.7 [a]	49.7 ± 2.5	1093.1 ± 57.0 [b]
PCL + 5% BFH	49.6 ± 0.2	979.7 ± 2.5 [a]	55.0 ± 3.9	1213.1 ± 89.6 [b]
PVA (control)	nd	nd	nd	nd
PVA + 1% BFH	35.2 ± 1.2	808.2 ± 16.2 [c]	45.6 ± 4.1	999.8 ± 91.8 [b]
PVA + 2.5% BFH	34.3 ± 1.3	797.2 ± 19.1 [c]	54.4 ± 1.1	1199.8 ± 25.2 [b]
PVA + 5% BFH	38.7 ± 0.5	850.2 ± 6.4 [b]	76.3 ± 2.5	1694.2 ± 56.3 [a]

[1] Nanofibers functionalized with bioactive feather hydrolysate (BFH) at different concentrations (1, 2.5, and 5% BFH) were subjected to extraction protocol and evaluated for antioxidant activity. Data represent mean ± standard deviation of three independent experiments. [2] Values expressed as Trolox equivalents (TEAC). Different superscript letters denote significant differences within the same column. [3] nd = not detected.

The antioxidant activities obtained by either DPPH or ABTS methods in this work were similar to those observed in some nanofibers incorporating casein hydrolysates [25], antioxidant peptides [39], and even typical antioxidants, such as phenolic compounds [40]. However, higher ABTS scavenging values were observed for the PVA nanofibers containing 5% BFH. Moreover, the BFH was successfully applied for the development of electrospun nanofibers with either PCL or PVA, suggesting a broad range of applications for these materials. Both polymers are interesting for the development of bioactive nanomaterials because of their biocompatibility, biodegradability, good chemical and thermal stability, and non-toxic nature [41,42]. PCL is a hydrophobic polymer showing a slow biodegradation rate and high mechanical strength [41], while PVA is a hydrophilic polymer that provides good mechanical and thermal properties due to the formation of hydrogen bonds [42].

The release of active compounds from nanomaterials is controlled by the diffusion of the substance within the nanostructure and the external phase, with the chemical potential gradient being the key thermodynamic driving force for diffusion. Hydrogen bonds and electrostatic and hydrophobic interactions are the main forces that control the entrapment of bioactive compounds and/or may affect the assembly of polymer structure in nanomaterials, influencing the release profile [43]. Thus, the release rate is usually reliant on the properties of the polymer and the active substance.

3.3. Hemolytic Activity of Nanofibers

All nanofibers under study showed hemolytic activity below 3% (Supplementary Table S3). The test clearly shows the lysis of erythrocytes caused by the positive control Triton X-100, resulting in the reddish supernatant, while the negative control (PBS) and nanofibers encapsulating BFH did not produce any hemolysis; that is, intact red blood cells were collected after the assay (Supplementary Figure S4).

According to the American Society for Testing and Materials (ASTM F756-17, 2017) [44], a hemolysis rate of less than 5% is expected for materials that are considered safe, while toxic materials would present a hemolytic percentage greater than 5%. The determination of hemolytic properties in vitro has been used as a common and important method for the preliminary cytotoxicity evaluation of materials [45]. Similar to the results described here, other studies that have investigated the hemolytic activity of PVA or PCL nanofibers showed that this type of material often presents a low hemolysis rate [33,46].

Considering the absence of hemolytic activity and the highest antioxidant activity verified by the nanofibers formulated with 5% BFH, only this concentration was selected for further analysis.

3.4. Scanning Electron Microscopy

According to the SEM images, all nanofibers reveal a morphological appearance free of beads (polymer clusters) with adequate structural continuity (Figures 3 and 4). PVA and PCL are chemically different polymers, whose properties will define the interaction with BFH and the performance during electrospinning, reflecting the structural aspects of the nanofibers. Thus, the polymer nature and concentration and the addition of BFH have influenced the dimension of the nanofibers (Table 2), and, in some cases, the morphological appearance as well (Figures 3 and 4). The nanofibers composed of PVA had an average diameter smaller than the nanofibers made using PCL at both concentrations of 10% and 15%. The 10% PVA nanofiber containing BFH increased by about 100 nm in relation to the control (from 196 to 282 nm), while a very similar size was observed using 15% PVA (Table 2). In contrast, the incorporation of BFH increased the nanofiber size by approximately 3 times in relation to the control with 10% PCL, whereas a decrease in average diameter was observed when BFH was incorporated into 15% PCL nanofibers. The size and morphology of nanofibers can be influenced by several factors, including the processing parameters and properties of the polymer solution, such as the presence of additives, surface tension, viscosity, conductivity, and solvent volatility [22,23]. Peptides are usually charged in solution, affecting cone–jet formation during electrospinning [47]

and thereby interfering with the evaporation of the solvent, which may result in fibers with larger diameters [48]. Thus, it could be hypothesized that the higher peptide-to-polymer ratio in the spinning solution containing 5% BFH and 10% PCL might induce the production of wider nanofibers.

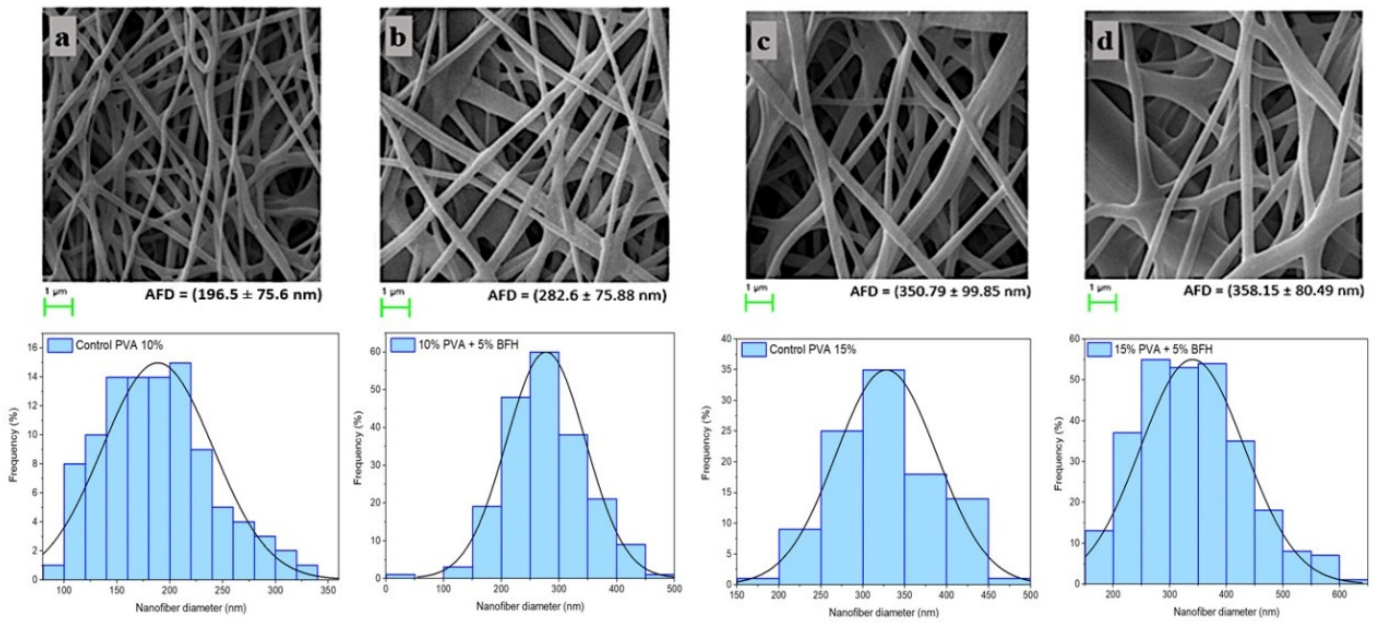

Figure 3. Scanning electron microscopy (upper panels) and histograms of diameter distribution (lower panels) of PVA nanofibers. Control 10% PVA (**a**), 10% PVA + 5% BFH (**b**), control 15% PVA (**c**), and 15% PVA + 5% BFH (**d**).

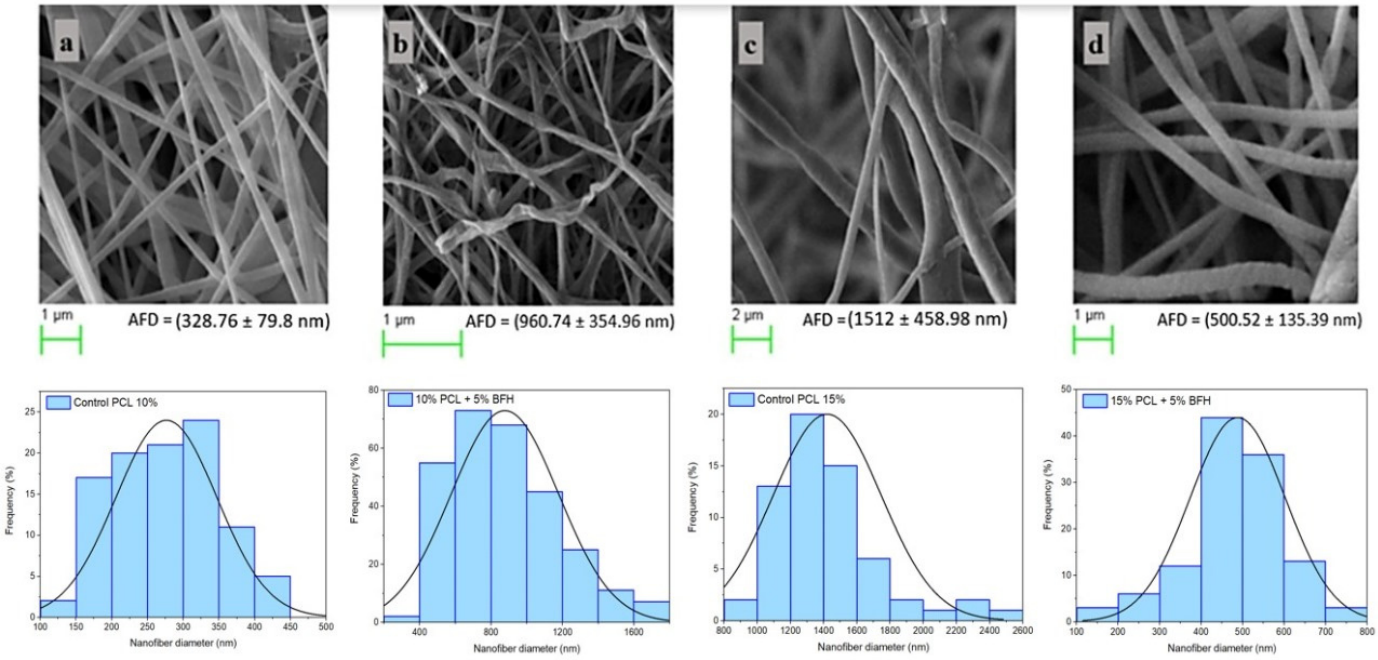

Figure 4. Scanning electron microscopy (upper panels) and histograms of diameter distribution (lower panels) of PCL nanofibers. Control 10% PCL (**a**), 10% PCL + 5% BFH, (**b**), control 15% PCL (**c**), and 15% PCL + 5% BFH (**d**).

Table 2. Average diameter of PVA and PCL nanofibers.

	Average Diameter (nm) [1]	
Formulation	**Control**	**5% BFH**
10% PVA	196.5 ± 75.6	282.6 ± 75.88
15% PVA	350.79 ± 99.85	358.15 ± 80.49
10% PCL	328.76 ± 79.8	960.74 ± 354.96
15% PCL	1512.0 ± 458.98	500.52 ± 135.39

[1] Data represent mean ± standard deviation of 100 fibers for each formulation measured using ImageJ v.1.51 software. Values were determined for nanofibers functionalized with bioactive feather hydrolysate (5% BFH) and control nanofibers (without BFH).

Similar values to that observed in this study have been reported for PVA/gelatin nanofibers, which showed around 290 nm in average diameter [38]. Control nanofibers produced with 13% PVA together with gelatin had an average size of 229 ± 26 nm, and, with the addition of active compounds (fluconazole/cinnamaldehyde), the size was increased to 334 ± 56 nm [49]. Other studies indicate that coaxial electrospinning allows the formation of PVA nanofibers with a smaller diameter; for example, using a spinning solution consisting of 20% PVA at an applied voltage of 28 kV resulted in nanofibers of 86.8 ± 7.4 nm [50]. The average diameter of PCL nanofibers also resembles the values described for PCL nanofibers formulated with lactobionic acid [33] and PCL/gelatin nanofibers incorporating curcumin-loaded zeolite nanoparticles [51].

The nanofibers manufactured using 10% of either PVA or PCL had average diameters in the nanometric range. Likewise, as the highest antioxidant activity was found for the nanofibers prepared with 10% PVA or PCL, further analyses were performed using this polymer concentration.

3.5. Thermal Analysis

The initial evaluation of TGA results reveals that PCL nanofibers have fewer thermal events than nanofibers made from PVA (Figure 5). The thermal degradation profiles of both PCL and PVA are consistent with the available literature [26,33,52,53]. The PVA nanofibers underwent thermal degradation in two steps (Figure 5a), while the thermograms of PCL nanofibers showed a single-step degradation profile, as the weight loss occurs more suddenly (Figure 5c). The thermal degradation of BFH resembled that observed for feather keratin, showing two stages of degradation, with a major weight loss from 200 to 400 °C and about a 75% weight loss after heating to 800 °C [54].

The analysis of PVA nanofibers showed that about 20% of the mass was maintained up to 400 °C, where another thermal degradation step takes place. With the last step, the maximum weight loss occurred at approximately 550 °C (Figure 5a). Similar to other studies, the first step of thermal degradation expected at temperatures lower than 100 °C is attributed to the loss of water, which is a characteristic of the thermal degradation of PVA nanofibers [46,52].

Basically, for the PCL nanofibers, there was a significant thermal degradation at about 430 °C, while for the nanofibers with the addition of BFH, the maximum weight loss was observed at approximately 400 °C (Figure 5c). This difference of about 30 °C reveals that the incorporation of BFH influenced the thermal properties of the PCL nanofibers. This suggests that the peptides present in BFH may interact with the PCL, influencing the packaging of polymer chains in comparison with the nanofibers prepared with pure polymer. In agreement with the TGA results of this study, PCL exhibited a single-step thermal degradation profile, starting at 346 °C and ending at 430 °C, with a maximum temperature of 390 °C and 0.5% residue at temperatures above 500 °C [53].

The DSC thermograms for PCL show an exothermic peak at approximately 55 °C (Figure 6a), which corresponds to the typical peaks described for PCL nanofibers [55,56]. The thermodynamic parameters Tm (melting temperature) and ΔHm (melting enthalpy) determined for PCL nanofibers were 58.9°C and 71.7 J/g, respectively, changing to 57.3 °C

and 60.1 J/g for BFH-containing nanofibers. These values were similar to those previously reported for PCL and PCL/chitosan fibers [57]. Otherwise, the DSC thermograms of PVA nanofibers did not show defined peaks (Figure 6b), similar to those described for amorphous systems containing proteins and/or polysaccharides [58]. In general, this behavior can be associated with the absence of microcrystalline interactions with macromolecules, resulting in amorphous materials [59]. The DSC thermogram for BFH showed an endothermic peak around 60–80 °C attributed to the water loss and a peak at 120–150 °C that could be due to peptide degradation (Supplementary Figure S3), similar to the peaks reported for keratin extracted from wool [60] and feathers [54].

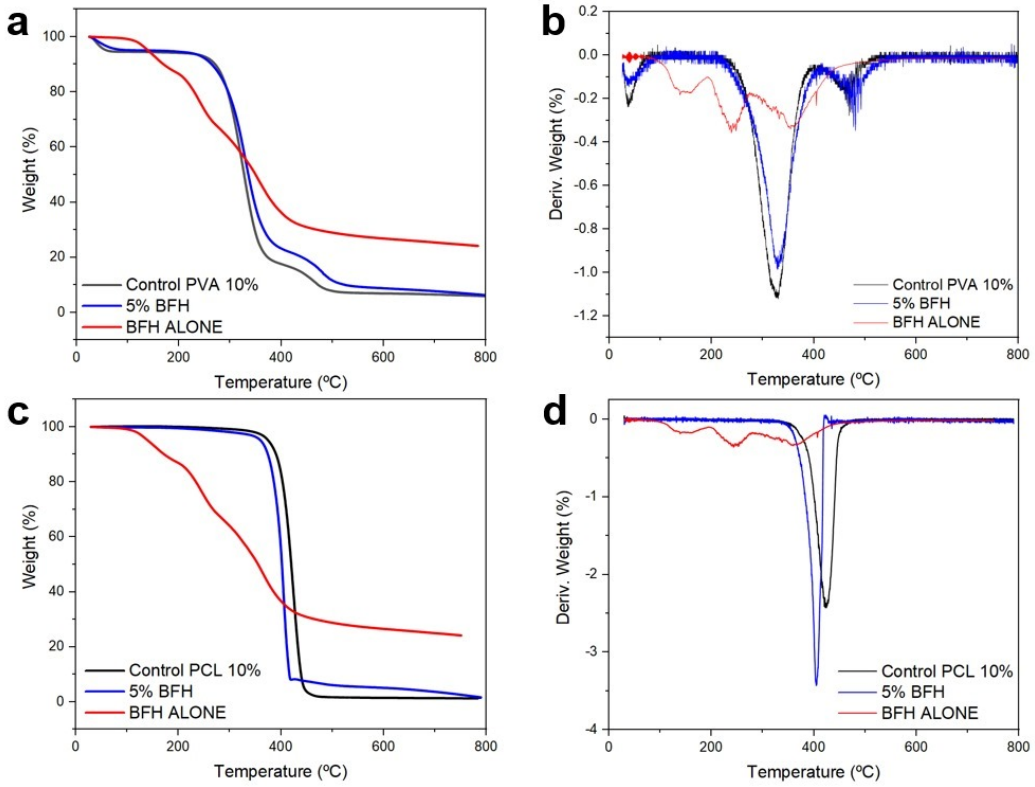

Figure 5. Thermogravimetric analysis of nanofibers. (**a**) TGA 10% PVA, (**b**) DTG 10% PVA, (**c**) TGA 10% PCL, and (**d**) DTG 10% PCL. The evaluation was performed in nanofibers functionalized with bioactive feather hydrolysate (5% BFH) and control nanofibers (without BFH).

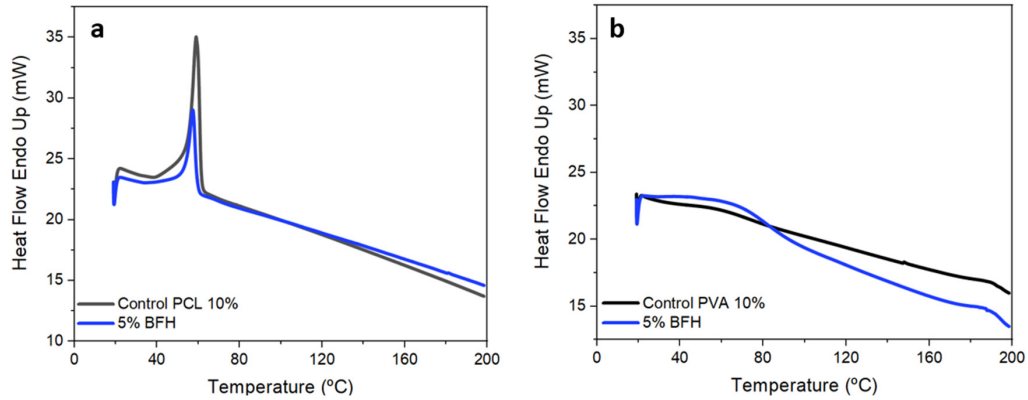

Figure 6. Differential scanning calorimetry (DSC) analysis of nanofibers composed of 10% PCL (**a**) and 10% PVA (**b**). The evaluation was performed in nanofibers functionalized with bioactive feather hydrolysate (5% BFH) and control nanofibers (without BFH).

3.6. Fourier Transform Infrared Spectroscopy (FTIR)

The typical peaks expected for the polymeric materials under study were observed in the FTIR analysis. The main groups indicated for nanofibers made of PVA (Figure 7a) are observed at 3304, 2940, 1716, 1420, and 1095 cm^{-1}, which are related to the stretching of OH groups, including free hydroxyl groups and inter/intramolecular hydrogen bonds, CH stretching, C = O stretching, CH bending, and C-O-C stretching, respectively [38,49,61]. An almost identical spectrum to that of pure PVA was perceived through the FTIR spectrum of PVA/gelatin [49], with the exception of the sharp peak at 1261 cm^{-1}, which was evident at 1251 cm^{-1} in this study.

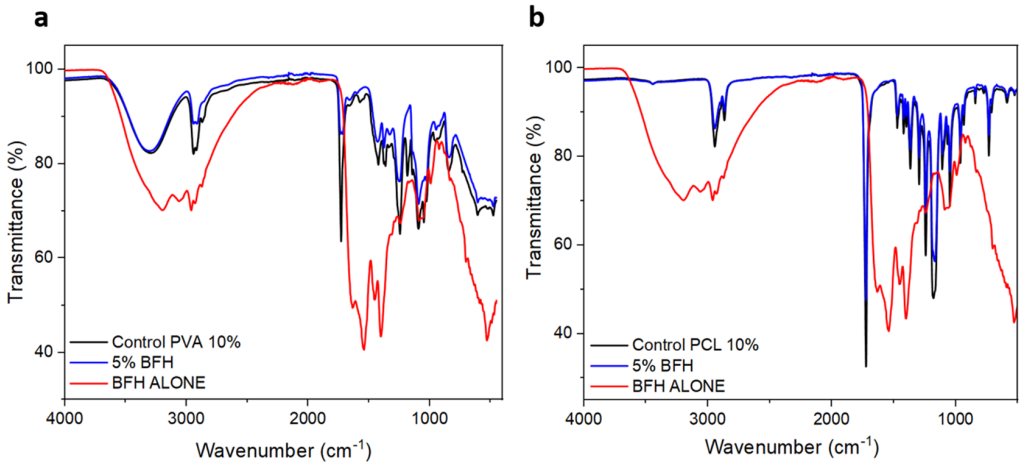

Figure 7. FTIR spectra of nanofibers composed of 10% PVA (**a**) and 10% PCL (**b**). The evaluation was performed in nanofibers functionalized with bioactive feather hydrolysate (5% BFH) and control nanofibers (without BFH).

Otherwise, PCL nanofibers have characteristic peaks of PCL (Figure 7b) observed at 2943 cm^{-1}, referring to the stretching vibration of the C-H bond, and the C=O group at 1740 cm^{-1}, which is typical carbonyl stretching. The peaks at 1170 cm^{-1} and 1240 cm^{-1} correspond to symmetric and asymmetric stretching of C-O-C, and the peak at 1293 cm^{-1} indicates the stretching of C=O and C-C [26,62].

The analysis of nanofibers composed of either PVA or PCL incorporating BFH revealed that the differences in FTIR spectra were mainly in the intensity of the peaks, probably because the signals from the hydrolysates were overlapped by signals from the polymer matrixes. FTIR analysis also indicates that no major structural changes occurred in the polymer matrix, suggesting the absence of newly formed chemical bonds between the polymers and BFH. The presence of absorption bands at 1600–1700, 1510–1580, and 1250–1350 cm^{-1} indicates the presence of amide I, amide II, and amide III, respectively, represented by smaller fragments of keratin peptides. Compared with typical protein spectra, the peaks observed at 1633.47, 1538.98, and 1241.85 cm^{-1} belonging to amide I, amide II, and amide III, respectively [38,63], could be found in the FTIR spectrum for BFH alone. The amide peaks originating from proteins undergo small changes in the different concentrations incorporated into the polymeric nanofibers [64].

3.7. Mechanical Properties

The mechanical tests conducted with the PCL nanofibers showed that the incorporation of BFH influenced Young's modulus since this parameter was reduced from 42.6 ± 7.7 MPa in control nanofibers to 21.1 ± 2.0 MPa in BFH-containing nanofibers (Figure 8a). However, no significant differences were observed for PVA nanofibers, indicating that the addition of BFH had a greater impact on the mechanical property of the PCL matrix. Regarding the results of tensile strength and elongation, both mechanical properties were reduced with the addition of BFH. For example, the PCL nanofibers showed an

elongation rate of 38.3 ± 5.1%, which was reduced to 15.6 ± 1.6% with the addition of BFH. For PVA nanofibers a decrease in the elongation at break was also observed when BFH was included in the formulation. The control nanofiber has an elongation rate of 102.9 ± 21.6, but when BFH was added to the polymer, the value was reduced to 40.1 ± 12.3% (Figure 8c).

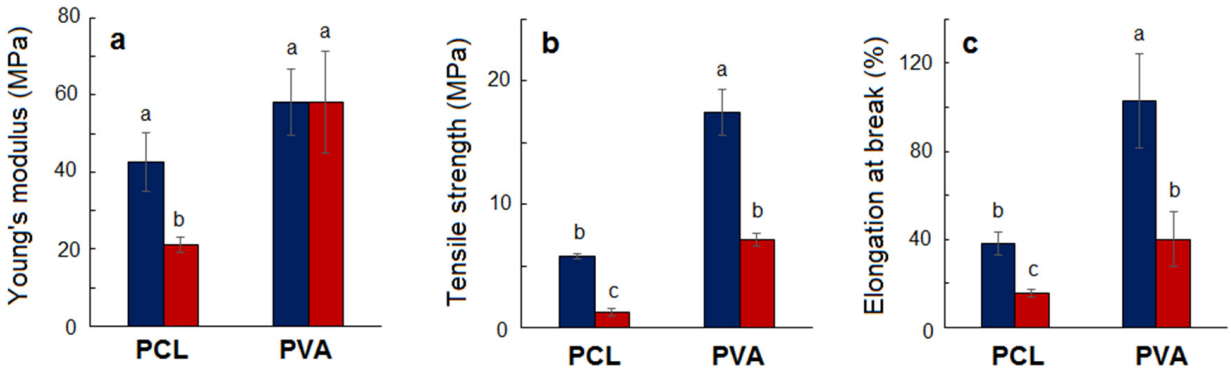

Figure 8. Mechanical properties of poly-ε-caprolactone (PCL) and poly(vinyl alcohol) (PVA) nanofibers. Values of Young's modulus (**a**), tensile strength (**b**), and elongation at break (**c**) were determined for control (blue bars) and functionalized nanofibers with 5% BFH (red bars). Data represent mean ± standard deviation of three independent experiments. Distinct letters indicate significant differences ($p < 0.05$).

The fiber diameter may interfere with the mechanical properties of nanofibers, and thinner PCL fibers are much stiffer than thicker ones [65]. This argument agrees with the results obtained in this study, where the nanofibers formulated with 10% PCL have an increased diameter with the addition of BFH, and a smaller Young's modulus in comparison with control nanofibers. The value observed with the incorporation of 5% BFH was similar to the modulus of 27.0 ± 4.6 MPa observed for PCL nanofibers with the addition of alginate [66]. Moreover, PCL nanofibers have an elongation capacity of 60%, which decreases to 20% when a curcumin additive is added [67]. Similarly, the elongation at break of PVA nanofibers is often reduced when other polymers or additives are included in the formulation [33,68,69].

The mechanical properties of nanofibers are essential for preliminary structural characterization. All possible applications of nanofibers, from active packaging, face masks, and surface coatings, in the biomedical field as a wound healing membrane depend on good properties in the structure of the material so that they successfully protect the active compounds.

4. Conclusions

Bioactive hydrolysates were produced via submerged cultivation with *Bacillus* sp. CL18. These hydrolysates have promising bioactive potential, considering the growing interest in natural antioxidant molecules. PVA and PCL nanofibers incorporating bioactive feather hydrolysates were produced, reaching ABTS radical scavenging activities of 76.3% (1694 μM TEAC) and 55.0% (1213 μM TEAC), respectively. These nanostructures also presented a hemolysis rate below 5%, indicating their potential as biocompatible materials. The nanofibers often showed a smooth morphology and average size in the nanometric range. The bioprocessing of poultry waste might represent an alternative to the disposal of feathers in a scenario where the valorization of byproducts is a crucial aspect of agro-industrial sustainability. The successful development of nanofibers incorporating feather hydrolysates obtained by microbial fermentation represents an advance toward the utilization of agro-industrial byproducts for the production of bioactive nanomaterials. However, specific studies involving scalability and detailed cost analysis should be conducted to validate the potential of this product.

Supplementary Materials: The following supporting information can be downloaded at https://www.mdpi.com/article/10.3390/fermentation10120615/s1, Figure S1: Production of proteases by *Bacillus* sp. CL18. The submerged cultures were carried out in feather broth containing 10 g/L of chicken feathers, over 7 days; Figure S2: SDS-PAGE analysis of BFH obtained from *Bacillus* sp. CL18 cultivation in whole feathers. The crude extract (culture supernatant), obtained after 5 days of cultivation in feather medium, was submitted to SDS-PAGE, using a 12% polyacrylamide gel.; Figure S3: Differential scanning calorimetry (DSC) analysis for the bioactive feather hydrolysate (BFH); Figure S4: Hemolysis assay. Images show the resulting supernatants after treatments with (a) Triton X-100, used as positive control, (b) PBS, used as negative control, (c) 10% PCL nanofibers, (d) 10% PVA nanofibers. Table S1: Antioxidant properties of poly(vinyl alcohol) (PVA) nanofibers functionalized with BFH; Table S2: Antioxidant properties of poly-ε-caprolactone (PCL) nanofibers functionalized with BFH. Table S3: Hemolytic activity of poly-ε-caprolactone (PCL) and poly(vinyl alcohol) (PVA) nanofibers.

Author Contributions: Conceptualization, A.B. and N.J.C.; methodology, N.J.C. and A.A.V.; validation, D.J.D.; formal analysis, N.J.C. and A.A.V.; investigation, N.J.C. and D.J.D.; writing—original draft preparation, N.J.C. and D.J.D.; writing—review and editing, A.B.; funding acquisition, A.B. All authors have read and agreed to the published version of the manuscript.

Funding: This research was funded by Conselho Nacional de Desenvolvimento Científico e Tecnológico (CNPq, Brazil), grant number 308880/2021-8.

Institutional Review Board Statement: Not applicable.

Informed Consent Statement: Not applicable.

Data Availability Statement: The original contributions presented in the study are included in the article/Supplementary Materials, further inquiries can be directed to the corresponding author.

Acknowledgments: The authors thank the Laboratory of Physical Analyses (LAPFA, UFRGS) for the technical support in conducting thermal and mechanical analyses, the Center of Microscopy and Microanalysis (CMM, UFRGS) for the technical support on electron microscopy, and M.Sc. Diogo Vargas de Oliveira for the maintenance of the electrospinning apparatus.

Conflicts of Interest: The authors declare no conflicts of interest.

References

1. Pope, M.; Borg, B.; Boyd, R.D.; Holzgraefe, D.; Rush, C.; Sifri, M. Quantifying the value of soybean meal in poultry and swine diets. *J. Appl. Poultry Res.* **2023**, *32*, 100337. [CrossRef]
2. Battacchi, D.; Verkerk, R.; Pellegrini, N.; Fogliano, V.; Steenbekkers, B. The state of the art of food ingredients' naturalness evaluation: A review of proposed approaches and their relation with consumer trends. *Trends Food Sci. Technol.* **2020**, *106*, 434–444. [CrossRef]
3. Barba, F.J. An integrated approach for the valorization of cheese whey. *Foods* **2021**, *10*, 564. [CrossRef] [PubMed]
4. Coppola, D.; Lauritano, C.; Palma Esposito, F.; Riccio, G.; Rizzo, C.; de Pascale, D. Fish waste: From problem to valuable resource. *Mar. Drugs* **2021**, *19*, 116. [CrossRef] [PubMed]
5. Callegaro, K.; Brandelli, A.; Daroit, D.J. Beyond plucking: Feathers bioprocessing into valuable protein hydrolysates. *Waste Manag.* **2019**, *95*, 399–415. [CrossRef]
6. Sadh, P.K.; Kumar, S.; Chawla, P.; Duhan, J.S. Fermentation: A boon for production of bioactive compounds by processing of food industries wastes (by-products). *Molecules* **2018**, *23*, 2560. [CrossRef]
7. Pereira, A.S.; Souza, C.P.L.; Franson, R.C.B.; Ferreira, T.F.; Amaral, P.F.F. From agri-food wastes to enzyme production: A systematic review with Methodi Ordinatio. *Waste Biomass Valor.* **2024**, *15*, 5843–5870. [CrossRef]
8. Tropea, A. Food waste valorization. *Fermentation* **2022**, *8*, 168. [CrossRef]
9. Aguilar-Paredes, A.; Valdés, G.; Araneda, N.; Valdebenito, E.; Hansen, F.; Nuti, M. Microbial community in the composting process and its positive impact on the soil biota in sustainable agriculture. *Agronomy* **2023**, *13*, 542. [CrossRef]
10. Malik, K.; Capareda, S.C.; Kamboj, B.R.; Malik, S.; Singh, K.; Arya, S.; Bishnoi, D.K. Biofuels production: A review on sustainable alternatives to traditional fuels and energy sources. *Fuels* **2024**, *5*, 157–175. [CrossRef]
11. Ruan, S.; Li, Y.; Wang, Y.; Huang, S.; Luo, J.; Ma, H. Analysis in protein profile, antioxidant activity and structure-activity relationship based on ultrasound-assisted liquid-state fermentation of soybean meal with *Bacillus subtilis*. *Ultrasonics Sonochem.* **2020**, *64*, 104846. [CrossRef] [PubMed]
12. Zhang, X.; Sun, X.; Li, W.; Huang, X.; Tao, L.; Li, T.; Li, S. In vitro and in vivo antioxidant activities of soy protein isolate fermented with *Bacillus subtilis* Natto. *J. Food Sci. Technol.* **2021**, *58*, 3199–3204. [CrossRef] [PubMed]

13. Begunova, A.V.; Savinova, O.S.; Glazunova, O.A.; Moiseenko, K.V.; Rozhkova, I.V.; Fedorova, T.V. Development of antioxidant and antihypertensive properties during growth of *Lactobacillus helveticus*, *Lactobacillus rhamnosus* and *Lactobacillus reuteri* on cow's milk: Fermentation and peptidomics study. *Foods* **2021**, *10*, 17. [CrossRef] [PubMed]
14. Solieri, L.; Valentini, M.; Cattivelli, A.; Sola, L.; Helal, A.; Martini, S.; Tagliazucchi, D. Fermentation of whey protein concentrate by *Streptococcus thermophilus* strains releases peptides with biological activities. *Process Biochem.* **2022**, *121*, 590–600. [CrossRef]
15. Xiao, X.; Liao, B.; Li, T.; Chen, Y.; Zhou, J.; Li, X.; Rao, H.; Li, W.; Bian, F.; Liu, Q.; et al. Fermentation of feathers with *Bacillus* sp. TC5 to simultaneous obtain keratinase and antioxidant-rich peptide products. *Biomass Conv. Bioref.* **2024**. [CrossRef]
16. de Menezes, C.L.A.; Boscolo, M.; da Silva, R.; Gomes, E.; da Silva, R.R. The Degradation of chicken feathers by *Ochrobactrum intermedium* results in antioxidant and metal chelating hydrolysates and proteolytic enzymes for staphylococcal biofilm dispersion. *3 Biotech* **2023**, *13*, 202. [CrossRef]
17. Gottardi, D.; Ciccone, M.; Siroli, L.; Lanciotti, R.; Patrignani, F. Use of *Yarrowia lipolytica* to obtain fish waste functional hydrolysates rich in flavoring compounds. *Fermentation* **2022**, *8*, 708. [CrossRef]
18. Liu, L.; Qin, J.; Lan, B.; Hu, X.; Liao, T.; Tian, X.; Wu, Z. Functional improvement and characterization of protein hydrolysates prepared by the fermentation of irradiated tilapia skin. *Food Bioprod. Process.* **2024**, *147*, 219–229. [CrossRef]
19. Martí-Quijal, F.J.; Khubber, S.; Remize, F.; Tomasevic, I.; Roselló-Soto, E.; Barba, F.J. Obtaining antioxidants and natural preservatives from food by-products through fermentation: A review. *Fermentation* **2021**, *7*, 106. [CrossRef]
20. Pedro, A.C.; Paniz, O.G.; Fernandes, I.d.A.A.; Bortolini, D.G.; Rubio, F.T.V.; Haminiuk, C.W.I.; Maciel, G.M.; Magalhães, W.L.E. The importance of antioxidant biomaterials in human health and technological innovation: A review. *Antioxidants* **2022**, *11*, 1644. [CrossRef]
21. Vilchez, A.; Acevedo, F.; Cea, M.; Seeger, M.; Navia, R. Applications of electrospun nanofibers with antioxidant properties: A review. *Nanomaterials* **2020**, *10*, 175. [CrossRef] [PubMed]
22. Zhang, J.; Yan, L.; Zhou, M.; Ma, J.; Wang, K.; Zhang, Y.; Drioli, E.; Cheng, X. Recent progress on functional electrospun polymeric nanofiber membranes. *Mater. Today Commun.* **2024**, *41*, 110530. [CrossRef]
23. Min, T.; Zhou, L.; Sun, X.; Du, H.; Zhu, Z.; Wen, Y. Electrospun functional polymeric nanofibers for active food packaging: A review. *Food Chem.* **2022**, *391*, 133239. [CrossRef] [PubMed]
24. Huang, K.; Si, Y.; Guo, C.; Hu, J. Recent advances of electrospun strategies in topical products encompassing skincare and dermatological treatments. *Adv. Colloid Interface Sci.* **2024**, 103236. [CrossRef]
25. Rajanna, D.; Pushpadass, H.A.; Emerald, F.M.E.; Padaki, N.V.; Nath, B.S. Nanoencapsulation of casein-derived peptides within electrospun nanofibres. *J. Sci. Food Agric.* **2022**, *102*, 1684–1698. [CrossRef]
26. Clerici, N.J.; Vencato, A.A.; Helm Júnior, R.; Daroit, D.J.; Brandelli, A. Electrospun poly-ε-caprolactone nanofibers incorporating keratin hydrolysates as innovative antioxidant scaffolds. *Pharmaceuticals* **2024**, *17*, 1016. [CrossRef]
27. Sobucki, L.; Ramos, R.F.; Daroit, D.J. Protease production by the keratinolytic *Bacillus* sp. CL18 through feather bioprocessing. *Environ. Sci. Pollut. Res.* **2017**, *24*, 23125–23132. [CrossRef]
28. Callegaro, K.; Welter, N.; Daroit, D.J. Feathers as bioresource: Microbial conversion into bioactive protein hydrolysates. *Process Biochem.* **2018**, *75*, 1–9. [CrossRef]
29. Lowry, O.H.; Rosebrough, N.J.; Farr, A.L.; Randall, R.J. Protein measurement with the Folin phenol reagent. *J. Biol. Chem.* **1951**, *193*, 265–275. [CrossRef]
30. Re, R.; Pellegrini, N.; Proteggente, A.; Pannala, A.; Yang, M.; Rice-Evans, C. Antioxidant activity applying an improved ABTS radical cation decolorization assay. *Free Rad. Biol. Med.* **1999**, *26*, 1231–1237. [CrossRef]
31. Brand-Williams, W.; Cuvelier, M.E.; Berset, C. Use of a free radical method to evaluate antioxidant activity. *LWT Food Sci. Technol.* **1995**, *28*, 25–30. [CrossRef]
32. Mosayebi, V.; Fathi, M.; Shahedi, M.; Soltanizadeh, N.; Emam-Djomeh, Z. Fast-dissolving antioxidant nanofibers based on *Spirulina* protein concentrate and gelatin developed using needleless electrospinning. *Food Biosci.* **2022**, *47*, 101759. [CrossRef]
33. Vencato, A.A.; Clerici, N.J.; Juchem, A.L.M.; Veras, F.F.; Rolla, H.C.; Brandelli, A. Electrospun nanofibers incorporating lactobionic acid as novel active packaging materials: Biological activities and toxicological evaluation. *Discover Nano* **2024**, *19*, 135. [CrossRef] [PubMed]
34. Bernardo, B.S.; Kopplin, B.W.; Daroit, D.J. Bioconversion of fish scales and feather wastes by *Bacillus* sp. CL18 to obtain protease and bioactive hydrolysates. *Waste Biomass Valor.* **2023**, *14*, 1045–1056. [CrossRef]
35. Gulsunoglu-Konuskan, Z.; Kilic-Akyilmaz, M. Microbial bioconversion of phenolic compounds in agro-industrial wastes: A review of mechanisms and effective factors. *J. Agric. Food Chem.* **2022**, *70*, 6901–6910. [CrossRef]
36. Ciurko, D.; Łaba, W.; Żarowska, B.; Janek, T. Enzymatic hydrolysis using bacterial cultures as a novel method for obtaining antioxidant peptides from brewers' spent grain. *RSC Adv.* **2021**, *11*, 4688–4700. [CrossRef]
37. Lemes, A.C.; Egea, M.B.; Oliveira Filho, J.G.d.; Gautério, G.V.; Ribeiro, B.D.; Coelho, M.A.Z. Biological approaches for extraction of bioactive compounds from agro-industrial by-products: A review. *Front. Bioeng. Biotechnol.* **2022**, *9*, 802543. [CrossRef]
38. He, S.; Jiang, L.; Liu, J.; Zhang, J.; Shao, W. Electrospun PVA/gelatin based nanofiber membranes with synergistic antibacterial performance. *Colloids Surf. A* **2022**, *637*, 128196. [CrossRef]
39. Hosseini, S.F.; Nahvi, Z.; Zandi, M. Antioxidant peptide-loaded electrospun chitosan/poly(vinyl alcohol) nanofibrous mat intended for food biopackaging purposes. *Food Hydrocoll.* **2019**, *89*, 637–648. [CrossRef]

40. Chuysinuan, P.; Thanyacharoen, T.; Techasakul, S.; Ummartyotin, S. Electrospun characteristics of gallic acid-loaded poly vinyl alcohol fibers: Release characteristics and antioxidant properties. *J. Sci. Adv. Mater. Devices* **2018**, *3*, 175–180. [CrossRef]
41. Thakur, M.; Majid, I.; Hussain, S.; Nanda, V. Poly(ε-caprolactone): A potential polymer for biodegradable food packaging applications. *Packag. Technol. Sci.* **2021**, *34*, 449–461. [CrossRef]
42. Zhang, W.; Khan, A.; Ezati, P.; Priyadarshi, R.; Sani, M.A.; Rathod, N.B.; Goksen, G.; Rhim, J.W. Advances in sustainable food packaging applications of chitosan/polyvinyl alcohol blend films. *Food Chem.* **2024**, *443*, 138506. [CrossRef] [PubMed]
43. Brandelli, A. Nanocomposites and their applications in antimicrobial packaging. *Front. Chem.* **2024**, *12*, 1356304. [CrossRef] [PubMed]
44. *ASTM F756-17*; Standard Practice for Assessment of Hemolytic Properties of Materials. American Standard for Testing Materials (ASTM): West Conshohocken, PA, USA, 2017.
45. Sæbø, I.P.; Bjørås, M.; Franzyk, H.; Helgesen, E.; Booth., J.A. Optimization of the hemolysis assay for the assessment of cytotoxicity. *Int. J. Mol. Sci.* **2023**, *24*, 2914. [CrossRef]
46. Phulmogare, G.; Rani, S.; Lodhi, S.; Patil, U.K.; Sinha, S.; Ajazuddin, S.; Gupta, U. Fucoidan loaded PVA/dextran blend electrospun nanofibers for the effective wound healing. *Int. J. Pharm.* **2024**, *650*, 123722. [CrossRef]
47. Bucci, R.; Georgilis, E.; Bittner, A.M.; Gelmi, M.L.; Clerici, F. Peptide-based electrospun fibers: Current status and emerging developments. *Nanomaterials* **2021**, *11*, 1262. [CrossRef]
48. Keirouz, A.; Wang, Z.; Reddy, V.S.; Nagy, Z.K.; Vass, P.; Buzgo, M.; Ramakrishna, S.; Radacsi, N. The history of electrospinning: Past, present, and future developments. *Adv. Mater. Technol.* **2023**, *8*, 2201723. [CrossRef]
49. Ilhan, E.; Cesur, S.; Sulutas, R.B.; Pilavci, E.; Dalbayrak, B.; Kaya, E.; Arisan, E.D.; Tinaz, G.B.; Sengor, M.; Kijeńska-Gawrońska, E.; et al. The role of multilayer electrospun poly(vinyl alcohol)/gelatin nanofibers loaded with fluconazole and cinnamaldehyde in the potential treatment of fungal keratitis. *Eur. Polym. J.* **2022**, *176*, 111390. [CrossRef]
50. Baykara, T.; Taylan, G. Coaxial electrospinning of PVA/Nigella seed oil nanofibers: Processing and morphological characterization. *Mater. Sci. Eng. B* **2021**, *265*, 115012. [CrossRef]
51. Jiang, B.; Yang, Z.; Shi, H.; Turki Jalil, A.; Mahmood Saleh, M.; Mi, W. Potentiation of curcumin-loaded zeolite Y nanoparticles/PCL-gelatin electrospun nanofibers for postsurgical glioblastoma treatment. *J. Drug Deliv. Sci. Technol.* **2023**, *80*, 104105. [CrossRef]
52. Cerqueira, G.R.C.; Gomes, D.S.; Victor, R.S.; Figueiredo, L.R.F.; Medeiros, E.S.; Neves, G.A.; Menezes, R.R.; Silva, S.M.L. Development of PVA/chitosan nanofibers by a green route using solution blow spinning. *J. Polym. Environ.* **2024**, *32*, 1489–1499. [CrossRef]
53. Darshan, T.G.; Chen, C.-H.; Kuo, C.-Y.; Shalumon, K.T.; Chien, Y.-M.; Kao, H.-H.; Chen, J.-P. Development of high resilience spiral wound suture-embedded gelatin/PCL/heparin nanofiber membrane scaffolds for tendon tissue engineering. *Int. J. Biol. Macromol.* **2022**, *221*, 314–333.
54. Sharma, S.; Gupta, A.; Kumar, A.; Kee, C.G.; Kamyab, H.; Saufi, S.M. An efficient conversion of waste feather keratin into ecofriendly bioplastic film. *Clean Technol. Environ. Policy* **2018**, *20*, 2157–2167. [CrossRef]
55. Kim, T.-H.; Kim, S.-C.; Park, W.S.; Choi, I.-W.; Kim, H.-W.; Kang, H.W.; Kim, Y.-M.; Jung, W.-K. PCL/gelatin nanofibers incorporated with starfish polydeoxyribonucleotides for potential wound healing applications. *Mater. Des.* **2023**, *229*, 111912. [CrossRef]
56. Ahmady, A.R.; Solouk, A.; Saber-Samandari, S.; Akbari, S.; Ghanbari, H.; Brycki, B.E. Capsaicin-loaded alginate nanoparticles embedded polycaprolactone-chitosan nanofibers as a controlled drug delivery nanoplatform for anticancer activity. *J. Colloid Interface Sci.* **2023**, *638*, 616–628. [CrossRef]
57. Zou, Y.; Zhang, C.; Wang, P.; Zhang, Y.; Zhang, H. Electrospun chitosan/polycaprolactone nanofibers containing chlorogenic acid-loaded halloysite nanotube for active food packaging. *Carbohydr. Polym.* **2020**, *247*, 116711. [CrossRef]
58. Matloub, A.A.; AbouSamra, M.M.; Salama, A.H.; Rizk, M.Z.; Aly, H.F.; Fouad, G.I. Cubic liquid crystalline nanoparticles containing a polysaccharide from *Ulva fasciata* with potent antihyperlipidaemic activity. *Saudi Pharm. J.* **2018**, *26*, 224–231. [CrossRef]
59. Shanks, R.A.; Gunaratne, L.M.W.K. Gelatinization and retrogradation of thermoplastic starch characterized using modulated temperature differential scanning calorimetry. *J. Therm. Anal. Calorim.* **2011**, *106*, 93–99. [CrossRef]
60. Okoro, O.V.; Jafari, H.; Hobbi, P.; Nie, L.; Alimoradi, H.; Shavandi, A. Enhanced keratin extraction from wool waste using a deep eutectic solvent. *Chem. Pap.* **2022**, *76*, 2637–2648. [CrossRef]
61. Chaudhary, P.K.; Saini, D.; Mishra, P.; Pandav, K.; Prasad, R. Essential oil active constituents loaded PVA nanofibers enhance antibiofilm activity against *Candida albicans* and *Candida tropicalis*. *J. Drug Deliv. Sci. Technol.* **2024**, *98*, 105871. [CrossRef]
62. Khasteband, M.; Sharifi, Y.; Akbari, A. Chrysin loaded polycaprolactone-chitosan electrospun nanofibers as potential antimicrobial wound dressing. *Int. J. Biol. Macromol.* **2024**, *263*, 130250. [CrossRef] [PubMed]
63. Yuan, Z.; Sheng, D.; Jiang, L.; Shafiq, M.; Khan, A.u.R.; Hashim, R.; Chen, Y.; Li, B.; Xie, X.; Chen, J.; et al. Vascular endothelial growth factor-capturing aligned electrospun polycaprolactone/gelatin nanofibers promote patellar ligament regeneration. *Acta Biomater.* **2022**, *140*, 233–246. [CrossRef] [PubMed]
64. Sengor, M.; Ozgun, A.; Gunduz, O.; Altintas, S. Aqueous electrospun core/shell nanofibers of PVA/microbial transglutaminase cross-linked gelatin composite scaffolds. *Mater. Lett.* **2020**, *263*, 127233. [CrossRef]

65. Alharbi, N.; Daraei, A.; Lee, H.; Guthold, M. The Effect of molecular weight and fiber diameter on the mechanical properties of single, electrospun PCL nanofibers. *Mater. Today Commun.* **2023**, *35*, 105773. [CrossRef]
66. Rashtchian, M.; Hivechi, A.; Bahrami, S.H.; Milan, P.B.; Simorgh, S. Fabricating alginate/poly(caprolactone) nanofibers with enhanced bio-mechanical properties via cellulose nanocrystal incorporation. *Carbohydr. Polym.* **2020**, *233*, 115873. [CrossRef]
67. Li, X.; Sun, S.; Yang, A.; Li, X.; Jiang, Z.; Wu, S.; Zhou, F. Dual-crosslinked methacrylamide chitosan/poly(ε-caprolactone) nanofibers sequential releasing of tannic acid and curcumin drugs for accelerating wound healing. *Int. J. Biol. Macromol.* **2023**, *253*, 127601. [CrossRef]
68. Ji, X.; Guo, J.; Guan, F.; Liu, Y.; Yang, Q.; Zhang, X.; Xu, Y. Preparation of electrospun polyvinyl alcohol/nanocellulose composite film and evaluation of its biomedical performance. *Gels* **2021**, *7*, 223. [CrossRef]
69. Cui, Z.; Zheng, Z.; Lin, L.; Si, J.; Wang, Q.; Peng, X.; Chen, W. Electrospinning and crosslinking of polyvinyl alcohol/chitosan composite nanofiber for transdermal drug delivery. *Adv. Polym. Technol.* **2018**, *37*, 1917–1928. [CrossRef]